HSP70-binding protein HSPBP1 regulates chaperone expression at a posttranslational level and is essential for spermatogenesis

Christian Rogon[a,*], Anna Ulbricht[a,*], Michael Hesse[b], Simon Alberti[a,†], Preethi Vijayaraj[c,‡], Diana Best[d], Ian R. Adams[d], Thomas M. Magin[c,§], Bernd K. Fleischmann[b], and Jörg Höhfeld[a]

[a]Institut für Zellbiologie and Bonner Forum Biomedizin, Rheinische Friedrich-Wilhelms-Universität Bonn, D-53121 Bonn, Germany; [b]Institut für Physiologie I, Life and Brain Centre, Rheinische Friedrich-Wilhelms-Universität Bonn, D-53105 Bonn, Germany; [c]Abteilung für Zellbiochemie, Institut für Biochemie und Molekularbiologie, Rheinische Friedrich-Wilhelms-Universität Bonn, D-53115 Bonn, Germany; [d]MRC Human Genetics Unit, MRC Institute of Genetics and Molecular Medicine, University of Edinburgh, Western General Hospital, Edinburgh EH4 2XU, United Kingdom

ABSTRACT **Molecular chaperones play key roles during growth, development, and stress survival. The ability to induce chaperone expression enables cells to cope with the accumulation of nonnative proteins under stress and complete developmental processes with an increased requirement for chaperone assistance. Here we generate and analyze transgenic mice that lack the cochaperone HSPBP1, a nucleotide-exchange factor of HSP70 proteins and inhibitor of chaperone-assisted protein degradation. Male *HSPBP1*$^{-/-}$ mice are sterile because of impaired meiosis and massive apoptosis of spermatocytes. HSPBP1 deficiency in testes strongly reduces the expression of the inducible, antiapoptotic HSP70 family members HSPA1L and HSPA2, the latter of which is essential for synaptonemal complex disassembly during meiosis. We demonstrate that HSPBP1 affects chaperone expression at a posttranslational level by inhibiting the ubiquitylation and proteasomal degradation of inducible HSP70 proteins. We further provide evidence that the cochaperone BAG2 contributes to HSP70 stabilization in tissues other than testes. Our findings reveal that chaperone expression is determined not only by regulated transcription, but also by controlled degradation, with degradation-inhibiting cochaperones exerting essential prosurvival functions.**

Monitoring Editor
Thomas Sommer
Max Delbrück Center for Molecular Medicine

Received: Feb 13, 2014
Revised: May 12, 2014
Accepted: May 23, 2014

INTRODUCTION

The 70-kDa heat shock proteins (HSP70s) and their regulating cochaperones constitute multifunctional cellular machineries essential for protein homeostasis (proteostasis; Mayer and Bukau, 2005; Brodsky and Chiosis, 2006; Vos *et al.*, 2008; Kampinga and Craig, 2010; Kettern *et al.*, 2010; Hartl *et al.*, 2011). Owing to their ability to bind hydrophobic protein sequences, HSP70s assist folding and assembly, conformational regulation, sorting, and degradation of client proteins. In the cytoplasm of mammalian cells, housekeeping functions are exerted by constitutively expressed HSPA8 (also known as HSC70 or HSP73; Vos *et al.*, 2008; Kampinga and Craig, 2010). Proteostasis capacity is increased under stressful conditions, such as heat or oxidative stress, by the expression of inducible HSP70s, including HSPA1A, HSPA1B, and HSPA1L (Vos *et al.*, 2008; Murphy, 2013). A cytoplasmic HSP70 family member with a restricted expression pattern is HSPA2 (HSP70-2), which was initially identified as a testis-specific chaperone essential for spermatogenesis (Dix *et al.*, 1996, 1997; Zhu *et al.*, 1997; Son *et al.*, 2000).

The process of spermatogenesis is a delicate and highly synchronized germ cell maturation pathway, which takes place in the seminiferous tubules of the testes (Russell *et al.*, 1990). The

This article was published online ahead of print in MBoC in Press (http://www.molbiolcell.org/cgi/doi/10.1091/mbc.E14-02-0742) on June 4, 2014.

*These authors contributed equally.

Present addresses: †Max Planck Institute of Molecular Cell Biology and Genetics, 01307 Dresden, Germany; ‡Department of Pediatrics, University of California, Los Angeles, Los Angeles, CA 90095; §Division of Cell and Developmental Biology, Translational Centre for Regenerative Medicine and Institute of Biology, University of Leipzig, 04103 Leipzig, Germany.

Address correspondence to: Jörg Höhfeld (hoehfeld@uni-bonn.de).

Abbreviations used: BAG, BCL2-associated athanogene; ES cell, embryonic stem cell; MEF, mouse embryonic fibroblast; MSCI, meiotic sex chromosome inactivation; SC, synaptonemal complex.

underlying developmental program places high demands on cellular homeostasis and is associated with a very active apoptosis machinery that serves to sort out unfit cells (Baum *et al.*, 2005; Shaha *et al.*, 2010; Okamoto *et al.*, 2014). In agreement with an important role of HSPA2 during sperm cell maturation, *HSPA2* transcription is strongly induced during early meiotic stages. Expression reaches a peak at pachytene, when the chaperone increasingly engages in the conformational regulation of signaling molecules and the disassembly of synaptonemal complexes (SCs) that connect paired, homologous chromosomes (Dix *et al.*, 1997; Zhu *et al.*, 1997). Targeted disruption of *HSPA2* causes sperm cell apoptosis and infertility in mice (Dix *et al.*, 1996), and decreased expression of the chaperone is also associated with male infertility in humans (Feng *et al.*, 2001). Thus spermatogenesis is critically dependent on chaperones such as HSPA2, and even mild stress conditions, such a hyperthermia, can trigger a massive demise of spermatocytes (Rockett *et al.*, 2001; Paul *et al.*, 2009).

More recent studies also identified HSPA2 in a range of cancer cells (Rohde *et al.*, 2005; Scieglinska *et al.*, 2011). This finding is remarkable because HSPA2 and also other inducible HSP70 chaperones display strong antiapoptotic activity and are required for cancer cell growth (Ravagnan *et al.*, 2001; Nylandsted *et al.*, 2004; Rohde *et al.*, 2005; Lanneau *et al.*, 2008). In general, tumorigenesis involves a series of molecular events allowing tumor cells to proliferate indefinitely and evade cellular safeguard mechanisms, such as apoptosis. This process of facilitated evolution increasingly leads to a dependence of the tumor cell on a specific set of oncogenes and nononcogenes (Luo *et al.*, 2009). The upregulated transcription of inducible HSP70 chaperones during tumorigenesis is one example of nononcogene dependence, which may in part be mediated by heat shock transcription factor 1 (HSF1; Dai *et al.*, 2007, 2012). Consistent with an important buffering role of chaperones during tumorigenesis, cancer treatment frequently relies on stress sensitization therapies, such as hyperthermia, to selectively kill off cancer cells. The strong parallels between spermatogenesis and tumorigenesis suggest that similar molecular mechanisms are at play. Indeed, misregulation of HSF1-dependent chaperone expression severely impairs spermatogenesis (Nakai *et al.*, 2000; Vydra *et al.*, 2006; Widlak *et al.*, 2007; Akerfelt *et al.*, 2010)

Chaperone-binding cochaperones confer functional specificity to the HSP70 chaperone system (Hartl *et al.*, 2011; Kampinga and Craig, 2010; Kettern *et al.*, 2010; Mayer and Bukau, 2005; Vos *et al.*, 2008). Engagement of HSP70s in protein degradation is triggered by cochaperones that act as chaperone-associated ubiquitin ligases and mediate the attachment of a ubiquitin-based degradation signal onto HSP70-bound client proteins (Kettern *et al.*, 2010). The founding member of these cochaperones is the carboxy-terminus of HSP70 interacting protein (CHIP), which triggers the degradation of a broad range of HSP70 clients (Arndt *et al.*, 2007). Of importance, CHIP-mediated ubiquitylation can direct clients either to the proteasome, a proteolytic complex specialized in the degradation of ubiquitylated proteins, or lysosomes, in a process called chaperone-assisted selective autophagy (Arndt *et al.*, 2010; Kettern *et al.*, 2010; Ulbricht *et al.*, 2013). Pathway selection is aided by additional cochaperones that enter the CHIP/HSP70 complex, by which members of the BCL2-associated athanogene (BAG) protein family are of particular importance (Takayama and Reed, 2001; Kettern *et al.*, 2010). BAG1 facilitates docking of the CHIP/HSP70 complex at the proteasome (Lüders *et al.*, 2000; Demand *et al.*, 2001), whereas BAG3 triggers lysosomal client degradation (Carra *et al.*, 2008; Gamerdinger *et al.*, 2009, 2011; Arndt *et al.*, 2010). Of note, the ubiquitin ligase activity of CHIP targets not only the bound client protein in the assembled complex. Instead, also BAG1, BAG3, HSPA8, and HSPA1A/B were shown to be modified by CHIP-mediated ubiquitylation (Jiang *et al.*, 2001; Alberti *et al.*, 2002; Arndt *et al.*, 2010). This mainly seems to provide additional sorting information for client degradation. However, in the case of inducible HSPA1A/B, CHIP-mediated ubiquitylation provides a means to initiate the degradation of the chaperone proteins themselves (Qian *et al.*, 2006). In this way, the cellular concentration of the chaperones is reduced when cells recover from stressful conditions and have to get rid of excess chaperone molecules (Qian *et al.*, 2006). This suggests that CHIP-mediated degradation contributes to the regulation of chaperone expression at a posttranslational level.

Chaperone cofactors can stimulate as well as restrict CHIP-mediated protein degradation. Restriction is mediated by the cochaperones HSPBP1 and BAG2. Binding of one of these cochaperones to the HSP70/CHIP complex inhibits the ubiquitin ligase activity of CHIP (Alberti *et al.*, 2004; Arndt *et al.*, 2005; Dai *et al.*, 2005). As a consequence, chaperone clients such as the CFTR ion channel are stabilized (Alberti *et al.*, 2004; Arndt *et al.*, 2005). Yet the full repertoire of chaperone clients affected by the CHIP inhibitors and their effect on organism development and homeostasis has not been established.

Here we show that HSPBP1 deficiency in mice causes male sterility because of impaired spermatogenesis and massive apoptosis of spermatocytes. We demonstrate that HSPBP1 exerts prosurvival functions by inhibiting the ubiquitylation and proteasomal degradation of inducible HSP70 family members. Finally, we provide evidence that the CHIP inhibitor BAG2 contributes to chaperone stabilization in tissues other than testes. Our study thus establishes a novel regulatory mechanism that controls the abundance of antiapoptotic, inducible members of the HSP70 chaperone family at a posttranslational level and in this way ensures the survival of cells that rely on high-level chaperone expression.

RESULTS

Targeted disruption of *HSPBP1* results in male sterility

In an effort to elucidate the physiological role of the HSP70 cochaperone and CHIP inhibitor HSPBP1, we investigated its expression profile in mice. Immunoblot analysis of tissue extracts with an anti-HSPBP1 antibody revealed weak to moderate expression of the cochaperone in brain, muscle, colon, and small intestine and strong expression in testis (Figure 1A). In situ hybridization was performed to identify HSPBP1-expressing cell types in testes. Antisense *HSPBP1* probes hybridized specifically to cells present inside the seminiferous tubules of the adult testes, with no staining in the somatic interstitial cells and no staining using the control sense *HSPBP1* probe (Figure 1B). The level of HSPBP1 expression varies among seminiferous tubule cross sections, depending on their epithelial stage, and is strongest in epithelial stages I–VI (Figure 1B; Russell *et al.*, 1990). Within the seminiferous tubules, HSPBP1 is expressed in the germ cells, with strongest expression in pachytene meiotic spermatocytes and postmeiotic round spermatids (Figure 1B). The expression pattern of HSPBP1 suggests that the cochaperone might have roles in meiosis and round spermatid differentiation during spermatogenesis.

To investigate the function of HSPBP1 for tissue development and homeostasis, we generated HSPBP1-deficient mice. For this purpose exons 2–4 of the *HSPBP1* locus, including the START codon (exon 2), were removed by targeted deletion in embryonic stem (ES) cells (Figure 1C). Mice were derived from these ES cells and backcrossed 10 times to C57BL/6 mice. Southern blot analysis of DNA isolated from ES cell clones and from obtained mice confirmed the

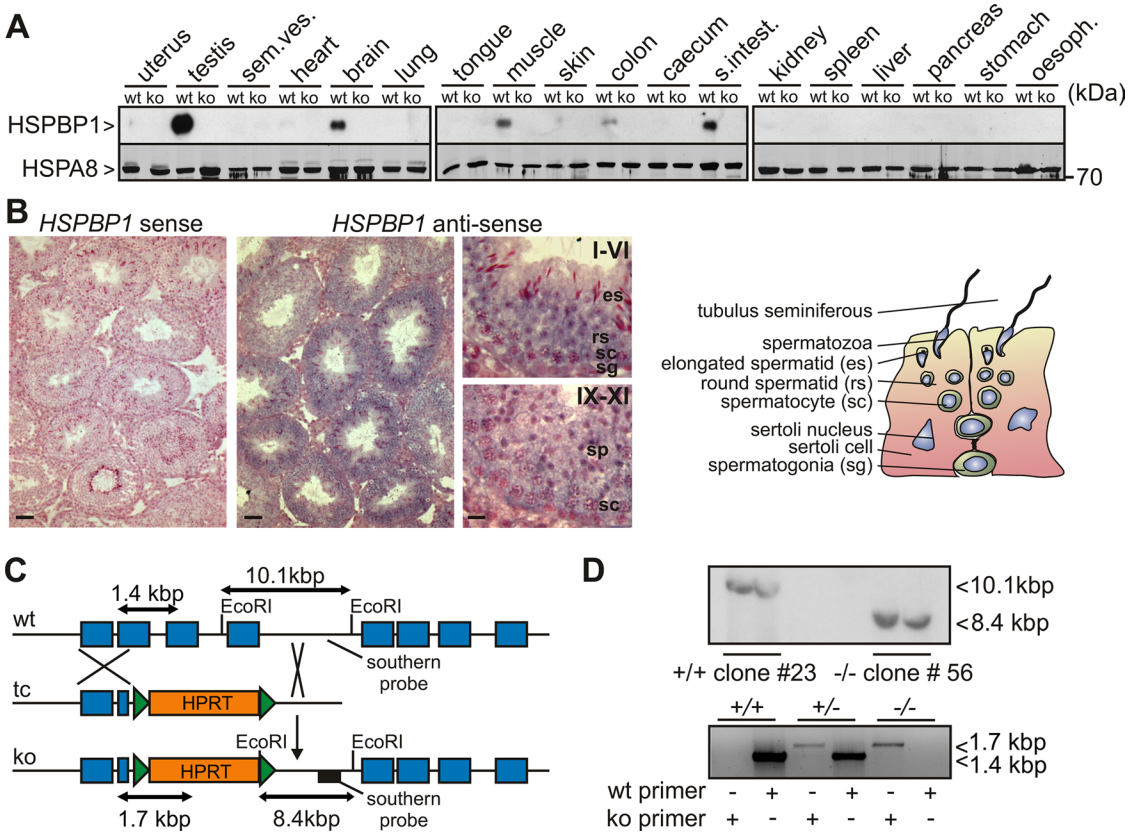

FIGURE 1: HSPBP1 is abundantly expressed in mouse testis. (A) Soluble lysates of the indicated tissues were prepared from 8-wk-old wild-type (wt) and HSPBP1 deficient (ko) mice. HSPBP1 and HSPA8 were detected using specific antibodies. Each lane corresponds to 100 µg of lysate protein. (B) In situ hybridization for *HSPBP1* in adult testis sections. Bound *HSPBP1* probe was visualized with dark blue/purple precipitate and sections counterstained with nuclear fast red. Scale bars, 50 µm (low magnification), 10 µm (high magnification). Seminiferous tubule stages are indicated by roman numerals, and examples of mitotic spermatogonia (sg), meiotic spermatocytes (sc), spermatids (sp), round spermatids (rs), and elongated spermatids (es) are annotated. (C) Schematic presentation of the disruption of the mouse *HSPBP1* locus by insertion of a targeting construct (tc). Blue boxes indicate exons of the *HSPBP1* gene. Regions detected during genotyping are shown. HPRT, hypoxanthine guanine phosphoribosyl transferase. (D) Genotyping of transgenic mice. Top, Southern blot analysis after digestion of DNA from ES cell clones with *Eco*RI. Bottom, PCR analysis using wt- and ko-specific primer pairs.

expected targeting of the *HSPBP1* gene, and a PCR was established to genotype pups (Figure 1D). The absence of the 40-kDa HSPBP1 protein in tissues of *HSPBP1*$^{-/-}$ mice was verified by immunoblot analysis (Figure 1A). *HSPBP1*$^{-/-}$ mice were born at normal Mendelian ratios and were largely indistinguishable from wild-type and heterozygous littermates. However, male *HSPBP1*$^{-/-}$ mice displayed a severe reduction in the size and weight of their testes, reaching only ~30% of the weight of *HSPBP1*$^{+/+}$ and *HSPBP1*$^{+/-}$ testes at an age of 8 wk (Figure 2, A and B). When mated, male but not female *HSPBP1*$^{-/-}$ mice were infertile, consistent with a severe impairment of testicular function (Table 1).

Seminiferous tubules of 8-wk-old wild-type and heterozygous mice were indistinguishable and contained spermatogenic cells in mitotic (spermatogonia), meiotic (spermatocytes) and postmeiotic (spermatids) phases of development (Figure 2C). In contrast, tubules of *HSPBP1*$^{-/-}$ mice displayed significant morphological alterations. Most tubules were highly vacuolized, whereas some appeared relatively intact but still lacked appreciable levels of round and elongated postmeiotic spermatids (Figure 2C). However, a number of cells remained at the basal region of the tubules, where mitotic spermatogonia and early meiotic spermatocytes are normally located (Figure 2C). The testis histology suggested that the infertility and reduced testis weight in *HSPBP1*$^{-/-}$ male mice are caused by a severe block in spermatogenesis. In agreement with this conclusion, epididymides of HSPBP1 deficient mice were devoid of mature spermatozoa (Figure 2D).

The histology of HSPBP1$^{-/-}$ testes revealed a severe reduction in the number of germ cells present within the seminiferous tubules. Cells in the adluminal region of vacuolized seminiferous tubules showed intense DNA staining and condensed nuclei, possibly reflecting apoptotic cell death (Figure 2C). A terminal deoxynucleotidyl transferase dUTP nick end labeling (TUNEL) assay that detects DNA strand breaks confirmed this notion. Whereas apoptotic cells were rare in seminiferous tubules of adult *HSPBP1*$^{+/+}$ mice, ~20% of the tubules in *HSPBP1*$^{-/-}$ mice contained multiple apoptotic cells (Figure 2E and F). Thus reduction in germ cell number in *HSPBP1*$^{-/-}$ testes is at least partly caused by increased cell death in these mutants.

To identify the stages of spermatogenesis that are defective in *HSPBP1*$^{-/-}$ testes, we investigated the expression of stage-specific differentiation markers. Expression of the spermatogonia/early spermatocyte marker DAZL (Ruggiu *et al.*, 1997) was largely unaffected in *HSPBP1*$^{-/-}$ testes (Figure 2G), suggesting that HSPBP1 deficiency does not impair the number of mitotic spermatogonia.

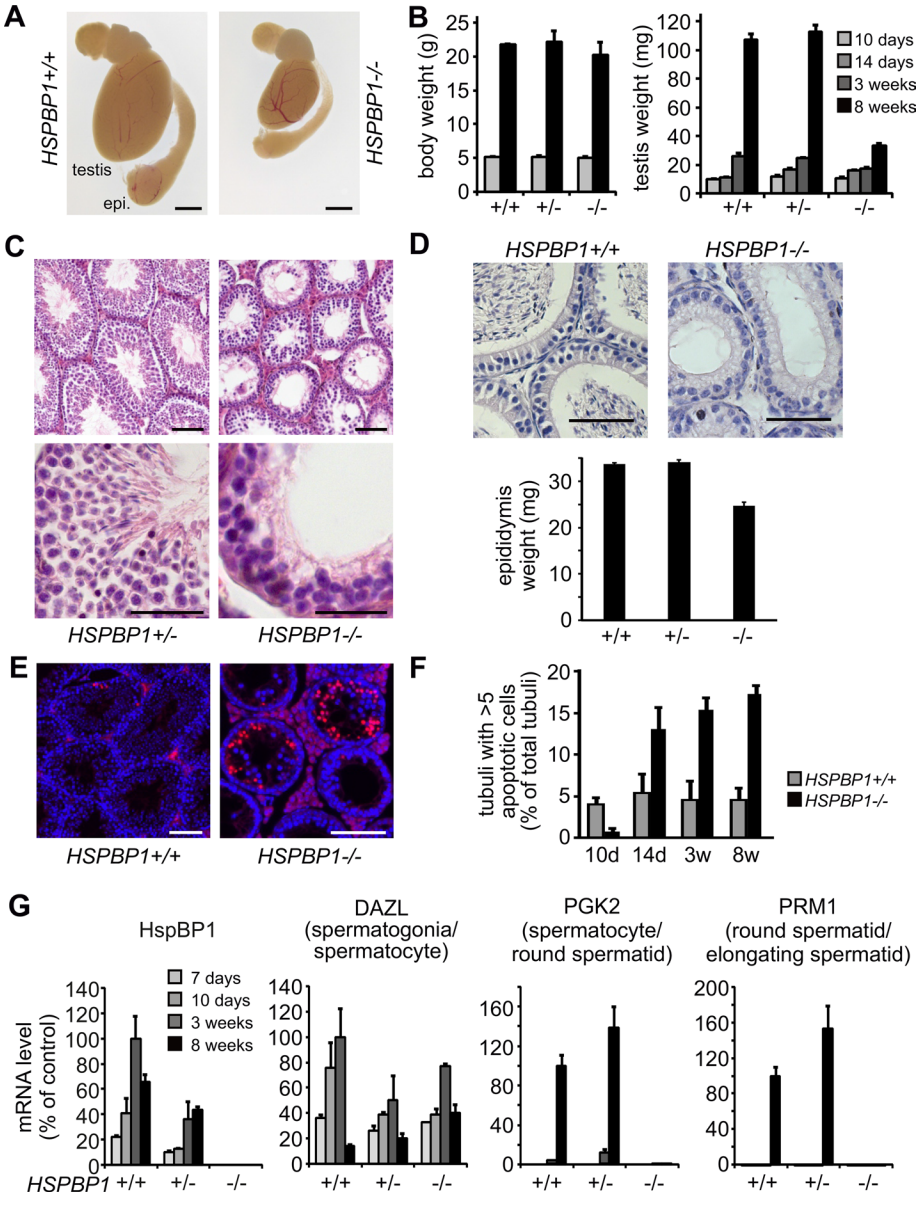

FIGURE 2: HSPBP1 is required for spermatogenesis. (A) Morphology of testes and epididymis (epi.) prepared from 8-wk-old wild-type (+/+) and HSPBP1-deficient mice (–/–). Scale bars, 2 mm. (B) Body weight and testis weight of wild-type (+/+) and transgenic mice heterozygous (+/–) and homozygous (–/–) for *HSPBP1* were determined at the indicated time points after birth. (C) Histological sections of testes of 8-wk-old *HSPBP1*$^{+/+}$ and *HSPBP1*$^{-/-}$ mice. Scale bars, 50 µm (low magnification), 20 µm (high magnification). (D) Epididymides of *HSPBP1*$^{-/-}$ mice are devoid of mature sperm and show reduced weight. Top, hematoxylin and eosin staining of epididymides sections from *HSPBP1*$^{+/+}$ and *HSPBP1*$^{-/-}$ mice. Scale bars, 50 µm. Bottom, epididymis weight was determined at 8 wk after birth (mean ± SEM, $n \geq 3$). (E) Seminiferous tubules in *HSPBP1*$^{-/-}$ mice show an increased number of apoptotic cells. TUNEL analysis of testes sections at 8 wk after birth. Scale bars, 50 µm. (F) Quantification of data obtained in E. (G) Transcript levels for HSPBP1 and stage-specific spermatogenesis markers determined in testis lysates by qRT-PCR at the indicated time points after birth. Maximum level detected in wild-type mice was set to 100% (mean ± SEM, $n \geq 3$).

In contrast, expression of phosphoglycerate kinase-2 (PGK2), a marker for meiotic spermatocytes/round spermatids (McCarrey *et al.*, 1992), and the postmeiotic spermatid marker PRM1 (Hecht *et al.*, 1985) were not detectable in testes of *HSPBP1*$^{-/-}$ mice (Figure 2G), revealing an inability of spermatocytes to progress through meiosis if HSPBP1 is missing. This is also consistent with timing of the appearance of the testicular weight phenotype during the first wave of spermatogenesis in prepubertal pups. *HSPBP1*$^{-/-}$ testes are similar in weight to control testes at 14 d postpartum (Figure 2B), a stage when mitotic spermatogonia and leptotene- and zygotene-stage meiotic spermatocytes are present (Bellve *et al.*, 1977). By 3 wk postpartum, as the first germ cells exit meiosis and become round spermatids, *HSPBP1*$^{-/-}$ testis weight is significantly lower than that of controls (Figure 2B).

To investigate the cause of germ cell apoptosis in *HSPBP1*$^{-/-}$ spermatocytes, we analyzed meiotic progression in chromosome spreads from adult testes (Figure 3). Chromosome spreads from *HSPBP1*$^{-/-}$ and *HSPBP1*$^{+/+}$ were immunostained for SYCP3, a component of the axial/lateral elements of the SC that labels this structure throughout meiotic prophase, and for SYCP1, a component of the transverse filaments of the SC that labels fully synapsed regions (Meuwissen *et al.*, 1992; Lammers *et al.*, 1994). Assembly of the axial element of the SC in leptotene and homologous chromosome synapsis and synaptonemal complex assembly in zygotene all appear to occur normally in *HSPBP1*$^{-/-}$ testes to generate fully synapsed pachytene nuclei (Figure 3A). However, no diplotene or later stages of meiosis were observed among a total of 300 SYCP3-positive meiotic spermatocytes derived from three *HSPBP1*$^{-/-}$ animals (Figure 3, A and B). In contrast, in control animals, 25% of SYCP3-positive spermatocytes were in the diplotene stage of meiosis, undergoing synaptonemal complex disassembly (Figure 3, A and B; $p < 0.01$, Fisher's exact test). Thus the spermatogenesis arrest in *HSPBP1*$^{-/-}$ testes appears to arise from a failure to progress beyond the pachytene stage of meiosis.

A number of mouse meiotic mutants have been described that exhibit apoptosis during pachytene as a response to defects in homologous chromosome synapsis (Burgoyne *et al.*, 2009). It has been proposed that the apoptotic response of these mutants is mediated by unrepaired autosomal DNA double-strand breaks sequestering the meiotic sex chromosome inactivation (MSCI) machinery away from the X and Y sex chromosomes (Burgoyne *et al.*, 2009). A second apoptosis-inducing checkpoint mechanism operating in pachytene spermatocytes appears to respond to stalled recombination intermediates (Li and Schimenti, 2007; Burgoyne *et al.*, 2009). Because SYCP3/SYCP1 immunostaining suggests that chromosome synapsis is not defective in *HSPBP1*$^{-/-}$ spermatocytes (Figure 3A), we tested whether the apoptosis in *HSPBP1*$^{-/-}$ spermatocytes might be a response to defects in meiotic recombination or MSCI. Immunostaining chromosome spreads for the dsDNA break marker γH2AX

♂	+/+	+/+	+/–	–/–	–/–
♀	+/+	–/–	–/–	–/–	+/+
Litter size ($n = 5$)	7.0	7.8	7.3	0	0

Values represent mean of five independent matings.

TABLE 1: Male HSPBP1-deficient mice are sterile.

(Mahadevaiah *et al.*, 2001) revealed that meiotic recombination is being initiated normally in leptotene in *HSPBP1*$^{-/-}$ testes and that these breaks are being processed and repaired on autosomes in zygotene and pachytene (Figure 3C). In addition, *HSPBP1*$^{-/-}$ spermatocytes acquire the late recombination marker MLH1 (Baker *et al.*, 1996), suggesting that recombination nodules are maturing correctly in pachytene (Figure 3D). Thus meiotic recombination appears to be progressing normally in *HSPBP1*$^{-/-}$ spermatocytes. Furthermore, the persistence of γH2AX staining on the X and Y chromosomes in pachytene (Figure 3C, arrow), suggests that the sex body is forming normally in *HSPBP1*$^{-/-}$ testes. We confirmed that MSCI is occurring in *HSPBP1*$^{-/-}$ testes by immunostaining chromosome spreads with antibodies to the Y-encoded RBMY protein (Turner *et al.*, 2002). Like *HSPBP1*$^{+/+}$ control spermatocytes, *HSPBP1*$^{-/-}$ spermatocytes are able to down-regulate expression of RBMY during pachytene (Figure 3E), suggesting that MSCI is occurring in these cells. Thus the meiotic prophase I arrest and apoptosis seen in *HSPBP1*$^{-/-}$ testes does not appear to be caused by overt defects in chromosome synapsis, the progression of meiotic recombination, or meiotic sex chromosome inactivation.

The presence of MLH1 foci in *HSPBP1*$^{-/-}$ spermatocytes indicates that these cells are progressing into mid/late pachytene (Figure 3D). To test whether *HSPBP1*$^{-/-}$ spermatocytes are dying during pachytene or progressing through to the end of pachytene, we assessed whether the proportion of early and mid/late pachytene cells differed between *HSPBP1*$^{+/+}$ and *HSPBP1*$^{-/-}$ testes. We quantified the proportion of early and mid/late pachytene spermatocytes in *HSPBP1*$^{-/-}$ testes by immunostaining chromosome spreads with SYCP3 and the mid/late pachytene marker histone H1t (Inselman *et al.*, 2003). Of interest, the proportion of histone H1t-positive pachytene nuclei was similar in chromosome spreads from *HSPBP1*$^{+/+}$ and *HSPBP1*$^{-/-}$ testes (132 of 300 *HSPBP1*$^{-/-}$ pachytene cells were H1t positive, compared with 135 of 300 *HSPBP1*$^{-/-}$ pachytene cells; Fisher's exact test, $p > 0.5$). Thus *HSPBP1*$^{-/-}$ spermatocytes apparently progress late into pachytene but do not appear to be able to enter diplotene. The late pachytene arrest in *HSPBP1*$^{-/-}$ testes presumably represents either a failure in meiotic progression at the late pachytene stage or a more direct defect in SC disassembly during diplotene.

Ablation of HSPBP1 impairs the expression of the inducible chaperones HSPA2 and HSPA1L in testes

The phenotype of *HSPBP1*$^{-/-}$ mice resembles the one observed after the ablation of the chaperone HSPA2, which is an HSP70 family member abundantly expressed in testes and localized to the synaptonemal complex in pachytene and diplotene spermatocytes (Allen *et al.*, 1996; Dix *et al.*, 1997). HSPA2 deficiency also results in defective synaptonemal complex disassembly, failed meiosis, germ cell apoptosis, and male infertility (Dix *et al.*, 1997; Alekseev *et al.*, 2009). Of note, HSPA2 was detectable in HSPBP1 complexes immunoprecipitated from wild-type testes lysates, suggesting that the chaperone and cochaperone form a functional HSP70 machinery in developing spermatocytes (Figure 4A). This is further supported by the fact that transcript levels for both proteins show a strong induction between 2 and 3 wk postpartum, when the first wave of

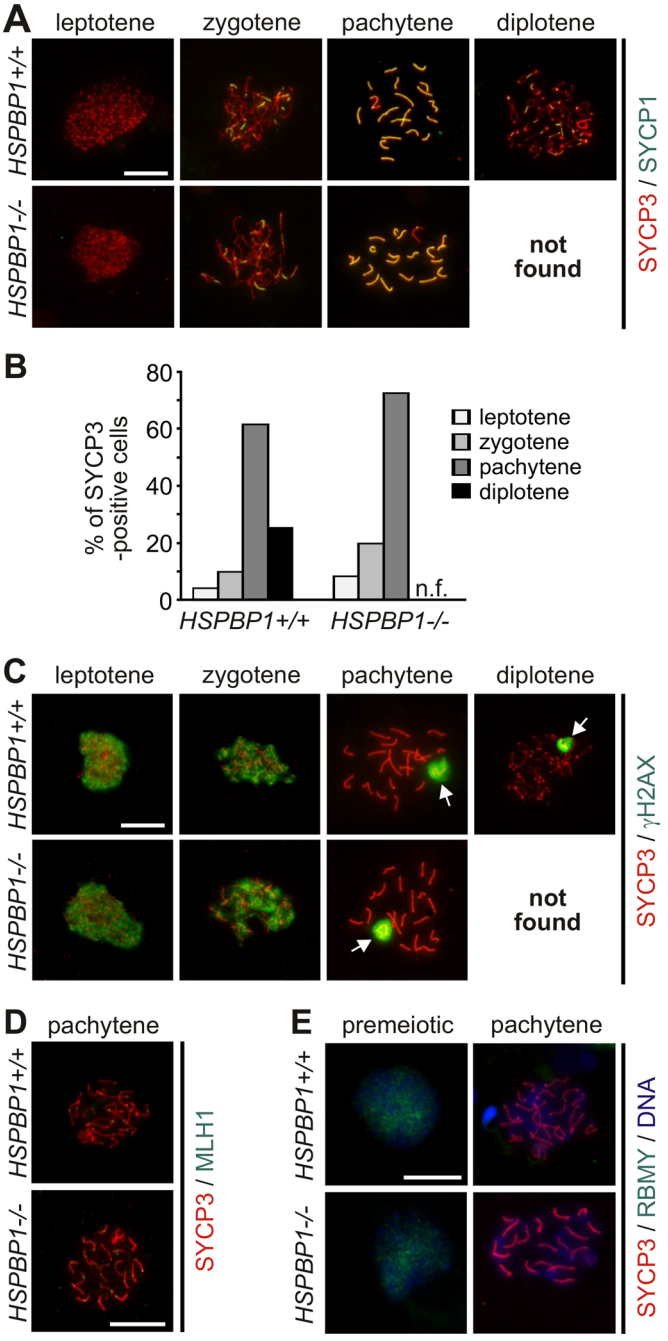

FIGURE 3: Ablation of HSPBP1 expression results in a late pachytene arrest of meiotic spermatocytes. (A) Immunostaining of chromosome spreads from adult testes for synaptonemal complex proteins SYCP3 (axial/lateral elements) and SYCP1 (transverse filament). (B) Graph showing the distribution of SYCP3-positive nuclei across meiotic prophase substages as determined by SYCP3/SYCP1 immunostaining ($n = 300$, three mice of each genotype, 100 nuclei/mouse). (C) Immunostaining of adult testis chromosome spreads for SYCP3 and γH2AX (double-stranded DNA-break marker). The sex body is indicated with an arrow. (D) Immunostaining of adult testis chromosome spreads for SYCP3 and MLH1 (late recombination marker). (E) Immunostaining of adult testis chromosome spreads for SYCP3 and RBMY (marker for meiotic sex chromosome inactivation). Scale bars, 20 μm.

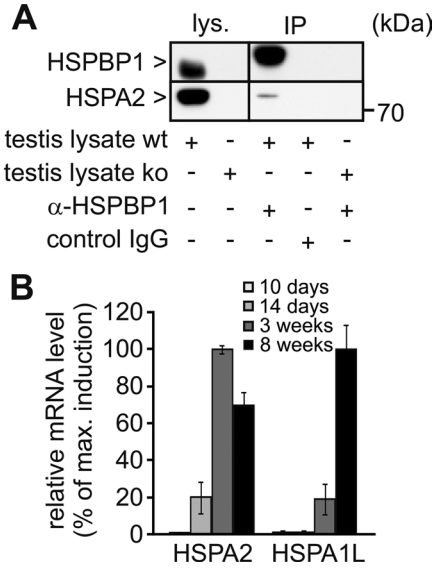

FIGURE 4: HSPBP1 and HSPA2 interact with each other in testes and are coinduced during spermatogenesis. (A) Testis lysates of wild-type (wt) and *HSPBP1*$^{-/-}$ mice (ko) were prepared in RIPA buffer, and the soluble protein fraction was subjected to immunoprecipitation (IP) with an anti-HSPBP1 antibody or the same amount of control immunoglobulin G. A 40-µg amount of lysate protein was loaded as control (lys.). (B) At the indicated time points after birth, mRNA was prepared from testis, and transcript levels were determined for HSPA2 and HSPA1L by qRT-PCR. The maximum transcript level was set to 100% (see Figure 2G for HSPBP1 expression during spermatogenesis).

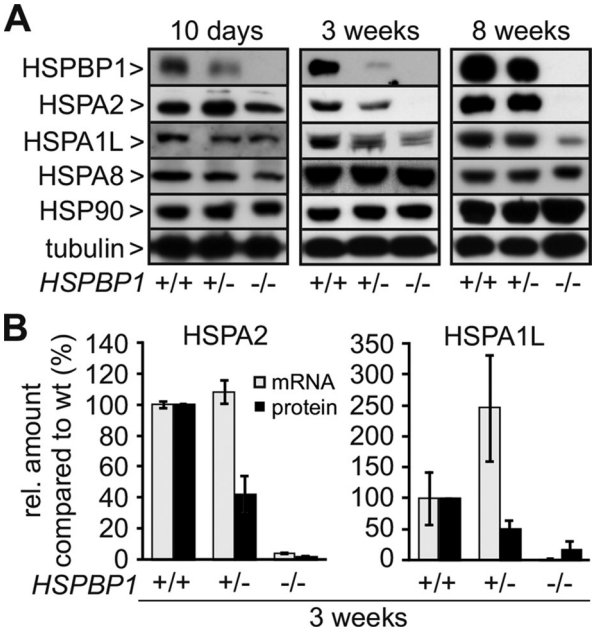

FIGURE 5: HSPBP1 ablation causes a reduction of HSPA2 and HSPA1L expression in mouse testis. (A) At the indicated time points after birth, testis lysates were prepared from wild-type (+/+) and HSPBP1-depleted mice. Chaperones and cochaperones were detected using specific antibodies. Each lane corresponds to 100 µg of soluble lysate protein. Tubulin served as loading control. (B) Protein levels of HSPA2 and HSPA1L, detected in testis lysates as shown in A, were quantified (black bars) and compared with transcript levels in testes for the two proteins determined by qRT-PCR (light gray) (mean ± SEM, $n \geq 3$).

spermatocytes progresses through pachytene and exits meiosis (Figures 2G and 4B).

In the course of these experiments we also investigated the expression of other inducible HSP70 family members in mouse testes. Whereas most cell types express HSPA1A and/or HSPA1B as main inducible forms (Vos *et al.*, 2008), we did not detect significant transcript levels for those two chaperones in testes. Instead, HSPA1L was identified as the main HSPA1 isoform expressed in this tissue, showing induced transcription between 2 and 3 wk postpartum (to ~20% of maximum level) and a strong further increase at later stages during spermatid maturation (Figure 4B).

Next we analyzed testis lysates for alterations in the chaperone/cochaperone network in the absence of HSPBP1. Although the cellular concentration of HSP90 and constitutively expressed HSPA8 remained largely unaffected, the lack of HSPBP1 had a strong effect on the expression of inducible HSP70s (Figure 5, A and B). HSPA2 was virtually absent in *HSPBP1*$^{-/-}$ testis at 3 and 8 wk postpartum, and HSPA1L levels were strongly reduced at these time points. It is conceivable that the altered cellular composition in *HSPBP1*$^{-/-}$ testis contributes to this decline in HSPA1L and HSPA2 levels, with spermatocytes no longer reaching stages of maximal chaperone expression because of massive apoptosis at late pachytene. Nevertheless, a dosage effect was observed in testes of heterozygous animals at 3 wk of age, when the reduced expression of HSPBP1 caused ~50% reduction in cellular concentration of HSPA2 and HSPA1L (Figure 5, A and B). Of note, levels of HSPA2 and HSPA1L transcripts did not show such a reduction and were instead increased in *HSPBP1*$^{+/-}$ heterozygous testes. These findings point to a role of HSPBP1 in the posttranslational stabilization of inducible HSP70s in spermatocytes.

HSPBP1 inhibits the ubiquitylation and proteasomal degradation of inducible HSP70 chaperones

We previously showed that HSPBP1 inhibits the activity of the HSP70-associated ubiquitin ligase CHIP in chaperone/cochaperone complexes (see later discussion of Figure 7; Alberti *et al.*, 2004). In these complexes, CHIP mediates not only the ubiquitylation of bound client proteins, but also that of associated chaperones and cochaperones (Jiang *et al.*, 2001; Alberti *et al.*, 2002; Qian *et al.*, 2006; Arndt *et al.*, 2010). This was shown to trigger the proteasomal degradation of inducible HSPA1A and HSPA1B but not of constitutively expressed HSPA8 (Jiang *et al.*, 2001; Qian *et al.*, 2006). The alterations of the chaperone repertoire observed in testes after HSPBP1 ablation may therefore directly reflect the CHIP-inhibiting activity of the cochaperone. In line with this conclusion, addition of purified HSPBP1 to in vitro ubiquitylation reactions significantly inhibited CHIP-mediated ubiquitylation of HSPA2 and HSPA1L (Figure 6, A–D).

The effect of HSPBP1 on proteasomal degradation of inducible HSP70s was investigated in human HeLa cells and mouse embryonic fibroblasts (MEFs). To separate regulated chaperone degradation from other stress responses, inducible chaperones were ectopically expressed under control of a cytomegalovirus promoter and specifically detected through an attached FLAG epitope. In HeLa cells, depletion of endogenous HSPBP1 by specific small interfering RNAs (siRNAs) led to ~50% reduction of HSPA1L expression, consistent with a stabilizing activity of the cochaperone (Figure 6E).

Mammalian cells also express the cochaperone BAG2, which shares with HSPBP1 the ability to inhibit CHIP-mediated ubiquitylation (Figure 7; Arndt *et al.*, 2005). We therefore investigated whether

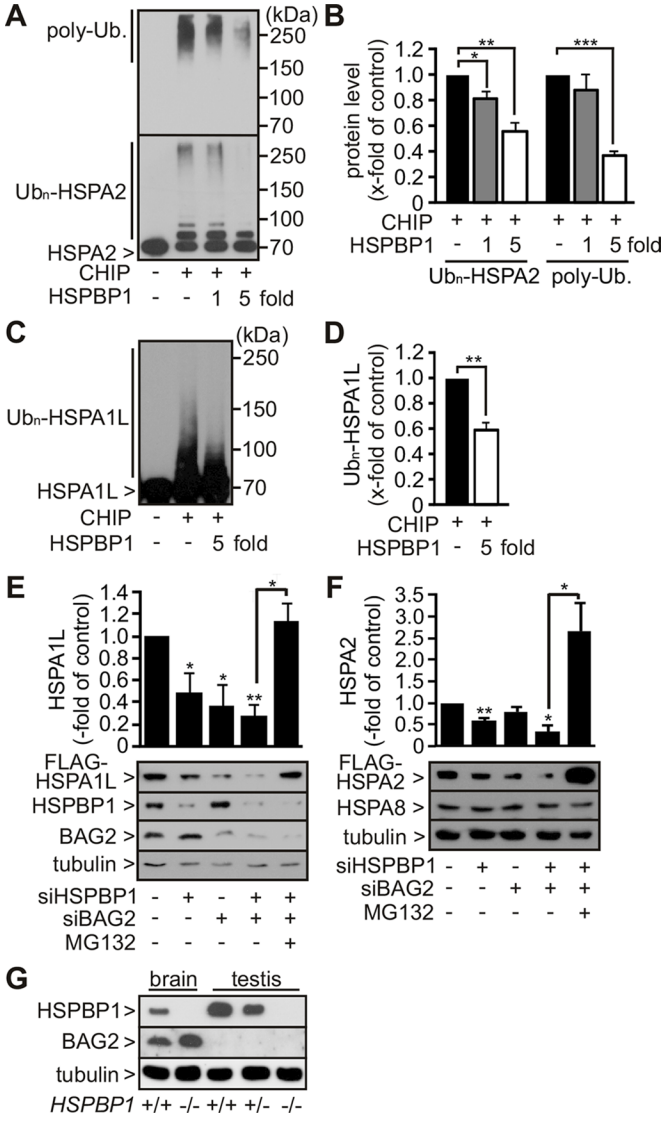

FIGURE 6: HSPBP1 interferes with the ubiquitylation of inducible HSP70 chaperones and cooperates with BAG2 in preventing the proteasomal degradation of HSPA2 and HSPA1L. (A) In vitro ubiquitylation of purified HSPA2 was performed in the presence of E1 and UBCH5b. Where indicated, purified CHIP and increasing concentrations of HSPBP1 (onefold and fivefold molar excess over added CHIP) were added to the reaction. Ubiquitin conjugates were detected by an anti-ubiquitin conjugate antibody (poly-Ub.) and anti-HSPA2 (HSPA2/Ub_n-HSPA2), respectively. (B) Quantification of data obtained in A (mean ± SEM, $n = 3$; *$p < 0.05$, **$p < 0.001$, ***$p < 0.0001$). (C) In vitro ubiquitylation of purified HSPA1L was performed in the presence of E1 and UBCH5b. Where indicated, purified CHIP and HSPBP1 (at a fivefold molar excess over added CHIP) were added to the reaction. Ubiquitin conjugates were detected by an anti-HSP70 antibody. (D) Quantification of data obtained in C (mean ± SEM, $n = 3$; **$p < 0.001$). (E) Analysis of HSPA1L stability in HeLa cells. FLAG-HSPA1L–expressing cells were transfected with siRNA targeting *HSPBP1* and *BAG2* or a control siRNA (–) as indicated. MG132 (20 μM, 16 h) was added when indicated to verify proteasomal degradation of FLAG-HSPA1L. Cells were harvested and lysed after 72 h and analyzed by SDS–PAGE and immunoblotting to quantify protein levels of FLAG-HSPA1L (mean ± SEM, $n = 3$; *$p < 0.05$, **$p < 0.001$). (F) Analysis of HSPA2 stability in mouse embryonic fibroblasts. FLAG-HSPA2–expressing cells were transfected with siRNA targeting *HSPBP1* and *BAG2* or a control siRNA (–) as indicated. MG132 (20 μM, 16 h) was added when indicated to verify proteasomal degradation. Cells were harvested and lysed after 48 h and analyzed by SDS–PAGE and immunoblotting to quantify protein levels (mean ± SEM, $n = 3$; *$p < 0.05$, **$p < 0.001$). (G) Detection of HSPBP1 and BAG2 in lysates of brain and testis from 3-wk-old wild-type (+/+), *HSPBP1* heterozygous (+/–), and homozygous (–/–) knockout mice. Each lane corresponds to 100 μg of soluble lysate protein. The cochaperones were detected with specific antibodies. Tubulin served as loading control.

BAG2 contributes to the stabilization of inducible HSP70 chaperones. Indeed, siRNA-mediated depletion of endogenous BAG2 from HeLa cells caused a reduction of HSPA1L expression to ~40% (Figure 6E). Moreover, when combined with HSPBP1 depletion, a further decrease in HSPA1L concentration was observed, suggesting cooperation of HSPBP1 and BAG2 in stabilizing inducible HSP70s. Finally, we demonstrated that cochaperone depletion did not affect HSPA1L expression in HeLa cells treated with the proteasome inhibitor MG132 (Figure 6E).

HSPA2 stability was analyzed in transiently transfected MEFs. Depletion of endogenous HSPBP1 led to ~50% reduction of HSPA2 expression, and codepletion of BAG2 further reduced chaperone levels to ~30%, which was not observed when proteasome activity was inhibited (Figure 6F). Furthermore, the cellular concentration of constitutively expressed HSPA8 was unaffected by cochaperone depletion (Figure 6F). Taken together, the data indicate that the CHIP inhibitors HSPBP1 and BAG2 jointly control the proteasomal degradation of inducible HSP70 chaperones in diverse mammalian cells.

Intriguingly, BAG2 was not detectable in mouse testis lysates, where HSPBP1 is very abundantly expressed (Figure 6G). In contrast, significant levels of BAG2 were found in brain homogenates that contain only moderate levels of HSPBP1. Furthermore, BAG2 levels were increased in *HSPBP1*$^{-/-}$ brains, most likely to compensate for the lack of the other CHIP inhibitor (Figure 6G). Thus we conclude that the cochaperones BAG2 and HSPBP1 regulate the expression of inducible HSP70s in a posttranslational and tissue-specific manner.

DISCUSSION

In this study, we identify a posttranslational mechanism that controls the cellular abundance of transcriptionally induced HSP70 family members. The two cochaperones HSPBP1 and BAG2 are of central importance in this regard. Both cochaperones were previously shown to inhibit the activity of the chaperone-associated ubiquitin ligase CHIP and restrict the degradation of Hsp70-bound client proteins (Figure 7A; Alberti *et al.*, 2004; Arndt *et al.*, 2005; Dai *et al.*, 2005; Kettern *et al.*, 2011). The findings presented here significantly extend this functional concept by identifying HSPBP1 and BAG2 as key regulators of inducible HSP70 expression (Figure 7B).

HSPBP1 specifically targets the HSP70 chaperones HSPA2 and HSPA1L, the expression of which is induced in testes during sperm development. HSPBP1 interferes with the CHIP-mediated ubiquitylation of both chaperones and thereby prevents their targeting for proteasomal degradation (Figure 6). Accordingly, HSPA2 and HSPA1L protein levels are strongly reduced in testis of *HSPBP1*$^{-/-}$ mice, and the phenotype of these mice phenocopies those reported for HSPA2-deficient animals (Dix *et al.*, 1996). In both cases, spermatocytes fail to disassemble the synaptonemal complex during meiosis I and arrest at late pachytene, followed by apoptotic cell death (Figure 2; Dix *et al.*, 1996). As a consequence, mice are unable to form mature sperm and display male infertility. Because HSPA2 and HSPA1L expression is induced at late stages of spermatogenesis, the strongly

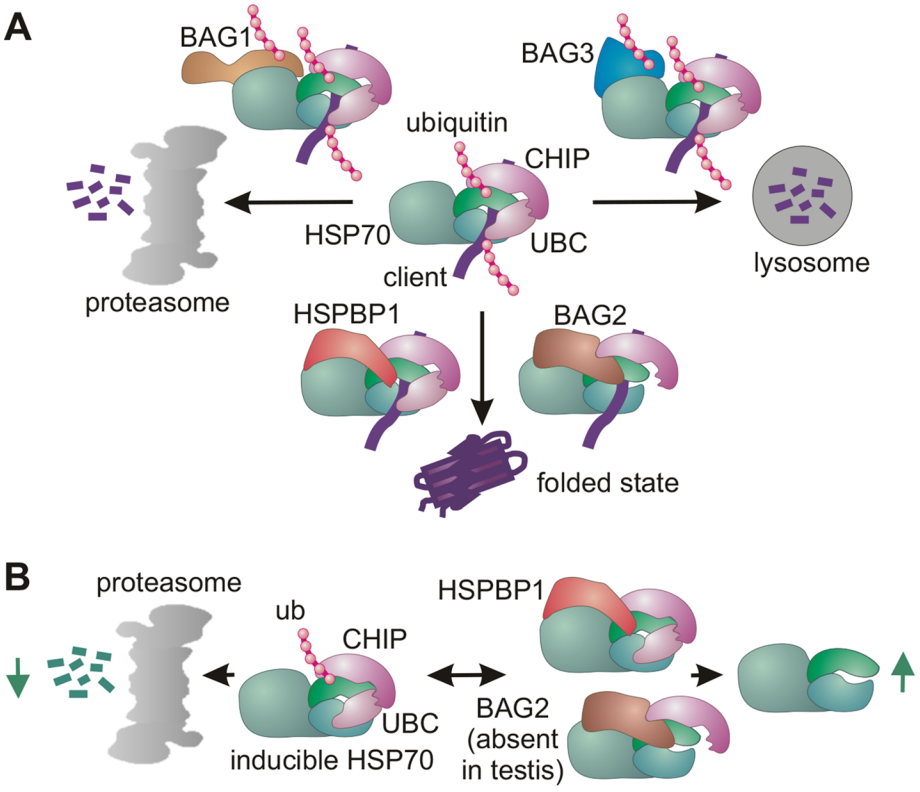

HSP70 member	transcription	ubiquitylated by CHIP	degraded by proteasome	stabilized by HSPBP1
HspA8	constitutive	yes (1)	no (1)	not affected*
HspA1A/B	inducible	yes (2)	yes (2)	n.d.
HspA1L	inducible	yes*	yes*	yes*
HspA2	inducible	yes*	yes (3)	yes*

FIGURE 7: Role of HSPBP1 and BAG2 as regulators of CHIP-mediated degradation. (A) Schematic presentation of the HSP70/cochaperone network that regulates CHIP-mediated protein degradation. CHIP binds to the carboxy terminus of HSP70 and ubiquitylates the chaperone and bound client proteins in conjunction with ubiquitin-conjugating enzymes of the UBCH4/5 family. Targeting to the proteasome is assisted by the cochaperone BAG1, whereas binding of BAG3 to the chaperone/CHIP complex induces the lysosomal degradation of the client. HSPBP1 and BAG2 inhibit the ubiquitin ligase activity of CHIP in the assembled chaperone complex and thereby facilitate the folding of the client. (B) Schematic presentation of the CHIP/HSPBP1/BAG2 cochaperone network that balances the expression of inducible HSP70 chaperones at the posttranslational level. CHIP is able to mediate the ubiquitylation of inducible HSP70s and induces their proteasomal degradation. Association of HSPBP1 or BAG2 with the HSP70/CHIP complex results in an inhibition of CHIP activity, leading to stabilization of inducible HSP70s. *Present study; (1) Jiang *et al.* (2001), (2) Qian *et al.* (2006), (3) Sasaki *et al.* (2008).

decreased number of postpachytene cells in *HSPBP1*$^{-/-}$ testes apparently contributes to the observed reduction in HSPA2 and HSPA1L levels. The effect of HSPBP1 on chaperone stability is therefore most evident in testes of heterozygous animals, in which apoptotic cell death is not increased but HSPA2 and HSPA1L protein levels are strongly reduced, whereas transcript levels are not similarly affected (Figure 5).

The role of HSPA1L in testes has not been elucidated in detail so far. In contrast, recent work revealed molecular details of HSPA2 function during spermatogenesis (Dix *et al.*, 1997; Zhu *et al.*, 1997; Alekseev *et al.*, 2009). It was shown that HSPA2 associates with the cyclin-dependent kinase CDC2 in testes and is required for the formation of an active CDC2/cyclin B kinase complex in pachytene spermatocytes, which drives the G2/M transition during meiosis I (Zhu *et al.*, 1997; Alekseev *et al.*, 2009). In addition, HSPA2 binds to SCs formed between paired homologous chromosomes during meiotic prophase and exerts essential functions during SC disassembly at diplotene (Dix *et al.*, 1997). As in *HSPA2*$^{-/-}$ testis, synaptonemal complexes formed normally in the absence of HSPBP1 but failed to disassemble, and normal diplotene spermatocytes were not observed in corresponding transgenic mice (Figure 3). The data presented here identify HSPA2 and HSPBP1 as a specific chaperone/cochaperone machinery required for the conformational regulation of signaling pathways and protein complex assembly/disassembly during male meiosis.

The chaperone machinery that drives male meiosis also comprises HSP90 proteins. Targeted disruption of HSP90α in mice results in a failure to mediate SC disassembly, followed by a late pachytene arrest of spermatogenesis and apoptotic death of spermatocytes, similar to findings for HSPBP1- and HSPA2-deficient mice, respectively (Grad *et al.*, 2010). In this regard, it is noteworthy that HSPBP1 acts not only as a CHIP inhibitor, but also as a nucleotide exchange factor of HSP70s, which triggers the release of bound client proteins by stimulating ADP–ATP exchange during the reaction cycle of the chaperones (Raynes and Guerriero, 1998; Shomura *et al.*, 2005). HSPBP1 may therefore facilitate the transfer of client proteins from HSPA2 onto HSP90 in meiotic spermatocytes. This may promote chaperone cooperation during the processing of clients that are targeted by both chaperones, including the previously mentioned kinase CDC2 (Zhu *et al.*, 1997; Grad *et al.*, 2010).

HSPBP1 is not the first cochaperone shown to be required for HSPA2 stabilization in testes. BAG6 (also known as BAT3), which, like BAG2, belongs to the BAG domain protein family (Takayama and Reed, 2001), was recently identified as an HSPA2-stabilizing cochaperone in meiotic spermatocytes (Sasaki *et al.*, 2008). Similar to HSPBP1, BAG6 prevents the ubiquitylation and proteasomal targeting of HSPA2. We therefore considered the possibility that BAG6 may also act as a CHIP inhibitor in ternary BAG6/HSP70/CHIP complexes. However, we observed that BAG6 is not detectable in CHIP complexes isolated from mammalian cells, and BAG6 binding to purified HSP70s actually blocks an association with CHIP (Huth and Höhfeld, unpublished results). This is consistent with findings from other labs that identified BAG6 as a component of a chaperone

machinery distinct from CHIP-containing complexes (Mariappan *et al.*, 2010; Wang *et al.*, 2011). BAG6 seems to stabilize HSPA2 in testes by preventing CHIP binding to the chaperone. In contrast, HSPBP1 inhibits the ubiquitylation activity of CHIP in assembled chaperone/cochaperone complexes, most likely by shielding lysine residues used for ubiquitin attachment (Alberti *et al.*, 2004). A hierarchy among the degradation-regulating cochaperones is indicated by the fact that BAG6 stabilizes HSPA2 but not HSPA1 forms in testes (Sasaki *et al.*, 2008), whereas HSPBP1 exerts a broader stabilizing function by preventing the degradation of HSPA2 and HSPA1L. Such differential effects could underlie a posttranslational fine tuning of the cellular chaperone repertoire.

HSPBP1-mediated stabilization of inducible HSP70s is not restricted to spermatocytes. In HeLa cells and MEFs, siRNA-triggered depletion of HSPBP1 caused the proteasomal degradation of inducible HSP70s (Figure 7). Of note, HeLa cells contain yet another degradation-regulating cochaperone, namely BAG2. It shares with HSPBP1 the ability to inhibit CHIP in assembled chaperone/cochaperone complexes (Figure 7; Arndt *et al.*, 2005; Dai *et al.*, 2005). Depletion of BAG2 also led to destabilization of HSPA1L and HSPA2, and the most pronounced effect on chaperone stability was observed when both cochaperones were simultaneously depleted (Figure 6). It seems that HSPBP1 and BAG2 jointly regulate the abundance of inducible HSP70s by inhibiting CHIP-mediated proteasomal targeting. Indeed, both cochaperones were detectable in brain homogenates from mice, and BAG2 expression was increased in *HSPBP1*$^{-/-}$ brains, most likely as a compensatory mechanism (Figure 6). On the other hand, BAG2 was not detectable in testes, which is consistent with the observed testes-specific phenotype of *HSPBP1*$^{-/-}$ mice. Although BAG2 could compensate for the loss of HSPBP1 in other tissues, it cannot do so in testes because it is not expressed there, thus making the male reproductive organ particularly prone to HSPBP1 ablation.

We previously observed that *HSPBP1*$^{-/-}$ mice show increased ubiquitylation and aggregation of antigens in bone marrow–derived dendritic cells, which is dependent on CHIP (Kettern *et al.*, 2011). The immune cells apparently also rely primarily on HSPBP1 for restricting CHIP-induced protein degradation. The effect on inducible chaperone expression in dendritic cells remains to be explored.

It is striking that HSPBP1 ablation affects inducible HSP70s but not constitutively expressed HSPA8 (Figure 6). However, this is consistent with previous observations that CHIP triggers the proteasomal degradation of inducible HSPA1A/B, whereas HSPA8 becomes also ubiquitylated by CHIP, but is not degraded by the proteasome (Figure 7B; Jiang *et al.*, 2001; Qian *et al.*, 2006). Accordingly, loss of HSPBP1 activity would be without consequence with regard to HSPA8 stability. The reason for this differential effect of CHIP on chaperone stability is elusive. It is conceivable that differences in the ubiquitylation pattern or the intrinsic folding propensity of the chaperone proteins affect their processing and unfolding at the proteasome, which is a prerequisite for the threading of substrates into the catalytic proteasomal core.

Is the differential treatment of constitutively and inducible HSP70 functionally important? HSPA1A, HSPA1B, and HSPA2, but not HSPA8, are overexpressed in many tumor cells and display strong antiapoptotic activity (Nylandsted *et al.*, 2000, 2004; Ravagnan *et al.*, 2001; Rohde *et al.*, 2005; Daugaard *et al.*, 2007b). It is striking that some tumor cells are strictly dependent on HSPA2, and selective depletion of HSPA2 in these cells induces a caspase-independent cell death pathway that involves lysosome permeabilization (Daugaard *et al.*, 2007a). The same process might contribute to spermatocyte apoptosis observed here upon HSPA2 depletion in *HSPBP1*$^{-/-}$ testis. In any case, our findings illustrate that the transcriptional induction of HSP70 expression during meiosis needs to be accompanied by cochaperone-mediated stabilization of HSP70 proteins in order to achieve sufficient chaperone buffering to ensure the survival of spermatocytes, which are, like tumor cells, dependent on high chaperone levels. The degradation-regulating cochaperone network may thus emerge as a promising therapeutic target in male infertility and cancer.

MATERIALS AND METHODS

Animal studies

Animal husbandry and all animal experimentation were carried out in compliance with German laws. Approval was obtained from the appropriate state and federal authorities (approval number: 9.93.2.10.31.07.247).

Generation of mutant mouse lines and genotyping

For inactivation of the *HSPBP1* locus, the targeting vector was constructed from a 129/ola mouse genomic library and designed to replace the first two exons of the *HSPBP1* gene, including the promoter region by the mouse hypoxanthine-phosphoribosyl-transferase (HPRT) minigene. The minigene was flanked by sequences homologous to the *HSPBP1* gene locus (short arm of homology, 1.4 kb; long arm of homology, 5 kb). The construct was cloned into a Bluescript II SK vector (Stratagene, Heidelberg, Germany) and electroporated into HM-1 ES cells (Magin *et al.*, 1998). Successful recombination was verified by Southern blotting, in which genomic DNA was digested with *Eco*RI and analyzed with Southern probes binding to a region flanking the deletion cassette insertion locus. Resulting positive ES cell clones were injected into C57/BL6/J blastocysts and transferred into C57/BL6/J mice. After successful germ line transmission, mice were maintained by breeding with C57/BL6/J. For genotyping, DNA was isolated from tail biopsies using the DNeasy Blood and Tissue Kit (Qiagen, Valencia, CA). Primers annealing to exons 2 and 3 of the *HSPBP1* locus were designed for the detection of wild-type loci, and primers targeting exon 2 and the deletion cassette were used to identify *HSPBP1*$^{-/-}$ mice.

Primers used for genotyping were as follows:

Exon 2 forward (+/+ and –/–): ACCTGCATTTACAGGCATCTG

Exon 3 reverse (+/+ only): CTTTGTCTGCCATGGACTTTC

Deletion cassette reverse (–/– only): AGCCTACCCTCTGGTAGATTG

Preparation and analysis of mouse tissues

For analysis of protein expression in different mouse tissues, respective organs from wild-type and *HSPBP1*$^{-/-}$ mice were dissected and shock-frosted in liquid nitrogen. Frozen samples were homogenized using a Potter tissue grinder and subsequently resolved in preheated SDS sample buffer (60°C) to a concentration of 100 mg/ml. Samples were boiled at 92°C for 10 min and centrifuged at 30,000 × *g* for 15 min for the removal of insoluble components. Resulting supernatants were analyzed by SDS–PAGE and Western blotting. The following primary antibodies were used: mouse anti-HSPBP1 (H98620; BD Biosciences, San Jose, CA), rabbit anti-HSPBP1 (FL-4; Delta Biolabs, Gilroy, CA), rabbit anti-HSPA2 (HPA000798; Atlas Antibodies, Stockholm, Sweden), rabbit anti-HSC70 (kindly provided by Ulrich Hartl, MPI for Biochemistry, Martinsried, Germany), mouse anti-HSC/HSP70 (SPA822; Enzo Life Sciences, Farmingdale, NY), rabbit anti-HSP70/HSPA1L (SPA812; Enzo Life Sciences), mouse anti-HSP90 (F-8; Santa Cruz Biotechnology, Santa Cruz, CA), rabbit anti-BAG2 (ab47106; Abcam, Cambridge, MA), mouse anti-FLAG

(M2; Sigma-Aldrich, St. Louis, MO), and mouse anti-tubulin (T5326; Sigma-Aldrich).

To analyze transcript levels, RNA from testes was isolated by first homogenizing shock-frosted organ samples in TRIzol (Life Technologies, Carlsbad, CA) using TissueLyser LT (Qiagen) with the addition of steel beads (4 or 7 mm). Vertical shaking was performed at 50 Hz for 7 min. DNA and RNA phases were separated by adding 200 µl of chloroform/ml of TRIzol. Subsequently isopropanol was added 1:1 to precipitate RNA from the corresponding phase. RNA was sedimented by centrifugation (30,000 × *g*, 20 min), washed in ethanol (70%), and dissolved in water (double distilled). An additional purification step was performed using the Qiagen RNA preparation kit for the removal of DNA contaminations. RNA concentration was measured and cDNA synthesis was performed using the SuperScript VILO cDNA Synthesis Kit (Life Technologies) according to the manufacturer's instructions. Quantitative real-time PCR (qRT-PCR) was performed with probe-based TaqMan GENE Expression Assays (Life Technologies) in real-time PCR cycler Rotor-Gene 6000 (Corbett/Qiagen). All samples were measured in triplet, and 18S RNA was used as reference gene. As negative control, cDNA was replaced by Ampuwa for each probe.

Histological examination

To analyze spermatogenesis in wild-type and *HSPBP1*$^{-/-}$ testes, hematoxylin/eosin (h/e) stainings were performed. Dissected testes were washed in phosphate-buffered saline (PBS) and fixed in 4% paraformaldehyde/PBS overnight at 4°C. Afterward, samples were washed in PBS and embedded in paraffin. Sections of 4 µm were cut and dehydrated for storage. For h/e staining of sections, samples were rehydrated and treated with Mayer's hematoxylin solution (Microm, Walldorf, Germany) for 1 min. Subsequently, sections were washed with water and incubated in eosin G solution (0.5% in water). After additional washing steps, sections were dehydrated again and mounted in Entellan (Merck, Whitehouse Station, NJ).

Apoptosis in testes of wild-type and *HSPBP1*$^{-/-}$ mice was estimated by TUNEL analysis of paraffin tissue sections (4 µm) that were obtained as described. After sample rehydration, ApopTag Red *InSitu* Apoptosis Detection Kit (Chemicon, Temecula, CA) was used according to manufacturer's instructions.

In situ hybridization

A plasmid containing mouse HSPBP1 (GenBank: BC014758.1) in pCMV-SPORT6 (Life Technologies) was used to generate sense and antisense digoxigenin-labeled RNA probes by in vitro transcription (Roche, Nutley, NJ). We hybridized 100 ng of probe to 7-µm wax sections of Bouin's fixed adult mouse testes at 50°C overnight as described (Best *et al.*, 2008). Bound probe was detected using alkaline phosphatase–conjugated anti-digoxigenin antibodies (Roche) and 5-bromo-4-chloro-3′-indolyphosphate/nitro blue tetrazolium substrate (Vector Labs, Burlingame, CA). Sections were counterstained with nuclear fast red. Seminiferous tubules were staged as described (Russell *et al.*, 1990).

Meiotic chromosome spreads

Chromosome spreads from adult testes were prepared essentially as described (Ollinger *et al.*, 2008). Briefly, one adult testis was homogenized and then resuspended in 1 ml of RPMI medium. One drop of cell suspension was incubated in 5 drops of 4.5% sucrose on a microscope slide for 1 h. Cells were lysed with 1 drop of 0.05% Triton X-100 for 10 min and fixed with 8 drops of fixing solution (2% paraformaldehyde, 0.02% SDS, pH 8.0) for 20 min. The slides were washed, blocked with 5% serum, 0.15% bovine serum albumin, and 0.1% Tween in PBS, and then incubated with primary antibodies, followed by secondary antibodies each for 1–2 h at room temperature. Primary antibodies were mouse anti-SYCP3 (1 µg/ml; Santa Cruz Biotechnology), rabbit anti-SYCP3 (1 µg/ml; Lifespan Biosciences, Seattle, WA), rabbit anti-SYCP1 (5 µg/ml; Abcam), rabbit anti-γH2AX (2 µg/ml; Millipore, Billerica, MA), mouse anti-MLH1 (5 µg/ml; BD Biosciences), guinea pig anti-histone H1t (1:1000 dilution; Mary Ann Handel, Jackson Laboratory, Bar Harbor, ME), and rabbit anti-RBMY (1:500 dilution; David Elliott, Newcastle University, Newcastle upon Tyne, United Kingdom). Alexa Fluor fluorescently labeled secondary antibodies were used at 1 µg/ml (Life Technologies), and DNA was stained with 2 µg/ml 4′,6-diamidino-2-phenylindole. For scoring meiotic progression and H1t-positive pachytene cells, 100 nuclei were scored from each of three wild-type and three HSPBP1$^{-/-}$ mice.

Immunoprecipitation of HSPBP1 complexes from testes

To characterize endogenous interaction between HSPBP1 and HSPA2, testes from wild-type and *HSPBP1*$^{-/-}$ mice were prepared as described and suspended in RIPA buffer (25 mM Tris-HCl, pH 8.0, 150 mM NaCl, 0.5% sodium deoxycholate, 1% Nonidet P-40, 10% glycerol, and 1× Complete Protease Inhibitor [Roche]). After 20 min of incubation, samples were centrifuged (30,000 × *g*, 30 min, 4°C), and protein concentrations were determined using Bradford reagent (Bio-Rad, Hercules, CA). Samples were adjusted to a concentration of 8 µg/µl. A 4-µg amount of antibody (specific against HSPBP1 or immunoglobulin G as control) was added to 80 µg of protein and incubated at 4°C on a spinning wheel overnight. Afterward, 20 µl of protein G–Sepharose was added to each sample, followed by incubation for another 6 h. Protein G–Sepharose pellets were washed seven times with RIPA buffer by successive centrifugation steps (1 min, 3000 rpm). Finally, Sepharose pellets were sedimented and boiled in 20 µl of SDS sample buffer (2 min, 92°C). The resulting supernatant was analyzed by SDS–PAGE and Western blotting.

In vitro ubiquitylation of HSP70 chaperones

Purified histidine (His)-HSPA2 at a final concentration of 1 µM was incubated with purified HSP40 (0.3 µM), UBCH5b (3 µM), CHIP (1 µM), E1 enzyme (0.1 µM), and ubiquitin (2.5 µg/µl) in ubiquitylation buffer (20 mM 3-(*N*-morpholino)propanesulfonic acid, pH 7.2, 100 mM KCl, 10 mM dithiothreitol, 5 mM ATP, 5 mM $MgCl_2$, 0.002% phenylmethylsulfonyl fluoride) in a final volume of 20 µl. Where indicated, purified HSPBP1 was added at a concentration of 1 or 5 µM, respectively. A sample without CHIP served as negative control. Samples were incubated for 30 min at 30°C and subsequently boiled in SDS sample buffer at 95°C for 3 min.

His-HSPA1L ubiquitylation was performed as described using HSP40 (0.06 µM), UBCH5b (0.6 µM), E1 enzyme (0.02 µM), and ubiquitin (0.5 µg/µl). The following primary antibodies were used for detection of ubiquitylated HSPA2 and HSPA1L: mouse anti-HIS-tag (MCA1396P; AbD Serotec, Raleigh, NC), rabbit anti-HSC70 (customized antibody generated by BioGenes GmbH, Berlin, Germany), and mouse anti-polyubiquitin (FK2; Biotrend, Destin, FL).

Analysis of HSP70 stability in HeLa and MEF cells

HeLa cells were transfected using jetPRIME transfection reagent (Peqlab, Wilmington, DE) according to the manufacturer's instructions. For the analysis of HSPA1L stability, cells were transfected with pCMV-Tag2B-*HSPA1L* for FLAG-HSPA1L expression and siRNA against *HSPBP1* and/or *BAG2* as indicated. Unspecific siRNA (Allstars; Qiagen) was used as negative control. Two days after

transfection, HSPBP1- and BAG2-depleted cells were treated with MG132 (20 μM, 16 h) to analyze proteasomal degradation of FLAG-HSPA1L. After 3 d, cells were harvested, lysed in RIPA buffer (25 mM Tris-HCl, pH 8.0, 150 mM NaCl, 0.5% sodium deoxycholate, 1% Nonidet P-40, 0.1% SDS, 10% glycerol, 1× Complete Protease Inhibitor), and incubated for 20 min on ice. Lysates were centrifuged at 30,000 × *g* for 20 min at 4°C. Supernatants were collected and analyzed by SDS–PAGE and Western blotting.

For the analysis of HSPA2 stability, MEF cells were transfected as described, using pCMV-Tag2B-*HSPA2* and respective siRNAs. MG132 treatment was performed after 36 h of transfection, and cells were subsequently harvested after 2 d. Lysis and Western blot analysis were performed as described.

The following primary antibodies were used: mouse anti-HSPBP1 (H98620; BD Biosciences), rabbit anti-BAG2 (ab47106; Abcam), mouse anti-FLAG (M2; Sigma-Aldrich), rabbit anti-HSPA8 (SAB2101098; Sigma-Aldrich), and mouse anti-tubulin (T5326; Sigma-Aldrich).

ACKNOWLEDGMENTS

We thank Karen Himmelberg for expert technical assistance, Mary Ann Handel and David Elliott for kind gifts of antibodies, and James Crichton (MRC Human Genetics Unit) for help with meiotic chromosome spread conditions. This work was supported by Deutsche Forschungsgemeinschaft Grants SFB 635 TP8 to J.H. and DFG FOR 1352 to B.K.F. (FL 276/7-1/2) and an intramural program grant to I.R.A. at the MRC Human Genetics Unit.

REFERENCES

Akerfelt M, Vihervaara A, Laiho A, Conter A, Christians ES, Sistonen L, Henriksson E (2010). Heat shock transcription factor 1 localizes to sex chromatin during meiotic repression. J Biol Chem 285, 34469–34476.

Alberti S, Bohse K, Arndt V, Schmitz A, Höhfeld J (2004). The cochaperone HspBP1 inhibits the CHIP ubiquitin ligase and stimulates the maturation of the cystic fibrosis transmembrane conductance regulator. Mol Biol Cell 15, 4003–4010.

Alberti S, Demand J, Esser C, Emmerich N, Schild H, Höhfeld J (2002). Ubiquitylation of BAG-1 suggests a novel regulatory mechanism during the sorting of chaperone substrates to the proteasome. J Biol Chem 277, 45920–45927.

Alekseev OM, Richardson RT, O'Rand MG (2009). Linker histones stimulate HSPA2 ATPase activity through NASP binding and inhibit CDC2/cyclin B1 complex formation during meiosis in the mouse. Biol Reprod 81, 739–748.

Allen JW, Dix DJ, Collins BW, Merrick BA, He C, Selkirk JK, Poorman-Allen P, Dresser ME, Eddy EM (1996). HSP70–2 is part of the synaptonemal complex in mouse and hamster spermatocytes. Chromosoma 104, 414–421.

Arndt V, Daniel C, Nastainczyk W, Alberti S, Höhfeld J (2005). BAG-2 acts as an inhibitor of the chaperone-associated ubiquitin ligase CHIP. Mol Biol Cell 16, 5891–5900.

Arndt V *et al*. (2010). Chaperone-assisted selective autophagy is essential for muscle maintenance. Curr Biol 20, 143–148.

Arndt V, Rogon C, Höhfeld J (2007). To be, or not to be—molecular chaperones in protein degradation. Cell Mol Life Sci 64, 2525–2541.

Baker SM *et al*. (1996). Involvement of mouse Mlh1 in DNA mismatch repair and meiotic crossing over. Nat Genet 13, 336–342.

Baum JS, St George JP, McCall K (2005). Programmed cell death in the germline. Semin Cell Dev Biol 16, 245–259.

Bellve AR, Cavicchia JC, Millette CF, O'Brien DA, Bhatnagar YM, Dym M (1977). Spermatogenic cells of the prepuberal mouse. Isolation and morphological characterization. J Cell Biol 74, 68–85.

Best D, Sahlender DA, Walther N, Peden AA, Adams IR (2008). Sdmg1 is a conserved transmembrane protein associated with germ cell sex determination and germline-soma interactions in mice. Development 135, 1415–1425.

Brodsky JL, Chiosis G (2006). Hsp70 molecular chaperones: emerging roles in human disease and identification of small molecule modulators. Curr Top Med Chem 6, 1215–1225.

Burgoyne PS, Mahadevaiah SK, Turner JM (2009). The consequences of asynapsis for mammalian meiosis. Nat Rev Genet 10, 207–216.

Carra S, Seguin SJ, Lambert H, Landry J (2008). HspB8 chaperone activity toward poly(Q)-containing proteins depends on its association with Bag3, a stimulator of macroautophagy. J Biol Chem 283, 1437–1444.

Dai Q *et al*. (2005). Regulation of the cytoplasmic quality control protein degradation pathway by BAG2. J Biol Chem 280, 38673–38681.

Dai C, Santagata S, Tang Z, Shi J, Cao J, Kwon H, Bronson RT, Whitesell L, Lindquist S (2012). Loss of tumor suppressor NF1 activates HSF1 to promote carcinogenesis. J Clin Invest 122, 3742–3754.

Dai C, Whitesell L, Rogers AB, Lindquist S (2007). Heat shock factor 1 is a powerful multifaceted modifier of carcinogenesis. Cell 130, 1005–1018.

Daugaard M, Kirkegaard-Sorensen T, Ostenfeld MS, Aaboe M, Hoyer-Hansen M, Orntoft TF, Rohde M, Jäättelä M (2007a). Lens epithelium-derived growth factor is an Hsp70-2 regulated guardian of lysosomal stability in human cancer. Cancer Res 67, 2559–2567.

Daugaard M, Rohde M, Jäättelä M (2007b). The heat shock protein 70 family: Highly homologous proteins with overlapping and distinct functions. FEBS Lett 581, 3702–3710.

Demand J, Alberti S, Patterson C, Höhfeld J (2001). Cooperation of a ubiquitin domain protein and an E3 ubiquitin ligase during chaperone/proteasome coupling. Curr Biol 11, 1569–1577.

Dix DJ, Allen JW, Collins BW, Mori C, Nakamura N, Poorman-Allen P, Goulding EH, Eddy EM (1996). Targeted gene disruption of Hsp70-2 results in failed meiosis, germ cell apoptosis, and male infertility. Proc Natl Acad Sci USA 93, 3264–3268.

Dix DJ, Allen JW, Collins BW, Poorman-Allen P, Mori C, Blizard DR, Brown PR, Goulding EH, Strong BD, Eddy EM (1997). HSP70-2 is required for desynapsis of synaptonemal complexes during meiotic prophase in juvenile and adult mouse spermatocytes. Development 124, 4595–4603.

Feng HL, Sandlow JI, Sparks AE (2001). Decreased expression of the heat shock protein hsp70-2 is associated with the pathogenesis of male infertility. Fertil Steril 76, 1136–1139.

Gamerdinger M, Hajieva P, Kaya AM, Wolfrum U, Hartl FU, Behl C (2009). Protein quality control during aging involves recruitment of the macroautophagy pathway by BAG3. EMBO J 28, 889–901.

Gamerdinger M, Kaya AM, Wolfrum U, Clement AM, Behl C (2011). BAG3 mediates chaperone-based aggresome-targeting and selective autophagy of misfolded proteins. EMBO Rep 12, 149–156.

Grad I, Cederroth CR, Walicki J, Grey C, Barluenga S, Winssinger N, De Massy B, Nef S, Picard D (2010). The molecular chaperone Hsp90alpha is required for meiotic progression of spermatocytes beyond pachytene in the mouse. PLoS One 5, e15770.

Hartl FU, Bracher A, Hayer-Hartl M (2011). Molecular chaperones in protein folding and proteostasis. Nature 475, 324–332.

Hecht NB, Bower PA, Kleene KC, Distel RJ (1985). Size changes of protamine 1 mRNA provide a molecular marker to monitor spermatogenesis in wild-type and mutant mice. Differentiation 29, 189–193.

Inselman A, Eaker S, Handel MA (2003). Temporal expression of cell cycle-related proteins during spermatogenesis: establishing a timeline for onset of the meiotic divisions. Cytogenet Genome Res 103, 277–284.

Jiang J, Ballinger CA, Wu Y, Dai Q, Cyr DM, Höhfeld J, Patterson C (2001). CHIP is a U-box-dependent E3 ubiquitin ligase: identification of Hsc70 as a target for ubiquitylation. J Biol Chem 276, 42938–42944.

Kampinga HH, Craig EA (2010). The HSP70 chaperone machinery: J proteins as drivers of functional specificity. Nat Rev Mol Cell Biol 11, 579–592.

Kettern N, Dreiseidler M, Tawo R, Höhfeld J (2010). Chaperone-assisted degradation: multiple paths to destruction. Biol Chem 391, 481–489.

Kettern N, Rogon C, Limmer A, Schild H, Höhfeld J (2011). The Hsc/Hsp70 co-chaperone network controls antigen aggregation and presentation during maturation of professional antigen presenting cells. PLoS One 6, e16398.

Lammers JH, Offenberg HH, van Aalderen M, Vink AC, Dietrich AJ, Heyting C (1994). The gene encoding a major component of the lateral elements of synaptonemal complexes of the rat is related to X-linked lymphocyte-regulated genes. Mol Cell Biol 14, 1137–1146.

Lanneau D, Brunet M, Frisan E, Solary E, Fontenay M, Garrido C (2008). Heat shock proteins: essential proteins for apoptosis regulation. J Cell Mol Med 12, 743–761.

Li XC, Schimenti JC (2007). Mouse pachytene checkpoint 2 (trip13) is required for completing meiotic recombination but not synapsis. PLoS Genet 3, e130.

Luo J, Solimini NL, Elledge SJ (2009). Principles of cancer therapy: oncogene and non-oncogene addiction. Cell 136, 823–837.

Lüders J, Demand J, Höhfeld J (2000). The ubiquitin-related BAG-1 provides a link between the molecular chaperones Hsc70/Hsp70 and the proteasome. J Biol Chem 275, 4613–4617.
Magin TM, Schroder R, Leitgeb S, Wanninger F, Zatloukal K, Grund C, Melton DW (1998). Lessons from keratin 18 knockout mice: formation of novel keratin filaments, secondary loss of keratin 7 and accumulation of liver-specific keratin 8-positive aggregates. J Cell Biol 140, 1441–1451.
Mahadevaiah SK, Turner JM, Baudat F, Rogakou EP, de Boer P, Blanco-Rodriguez J, Jasin M, Keeney S, Bonner WM, Burgoyne PS (2001). Recombinational DNA double-strand breaks in mice precede synapsis. Nat Genet 27, 271–276.
Mariappan M, Li X, Stefanovic S, Sharma A, Mateja A, Keenan RJ, Hegde RS (2010). A ribosome-associating factor chaperones tail-anchored membrane proteins. Nature 466, 1120–1124.
Mayer MP, Bukau B (2005). Hsp70 chaperones: cellular functions and molecular mechanism. Cell Mol Life Sci 62, 670–684.
McCarrey JR, Berg WM, Paragioudakis SJ, Zhang PL, Dilworth DD, Arnold BL, Rossi JJ (1992). Differential transcription of Pgk genes during spermatogenesis in the mouse. Dev Biol 154, 160–168.
Meuwissen RL, Offenberg HH, Dietrich AJ, Riesewijk A, van Iersel M, Heyting C (1992). A coiled-coil related protein specific for synapsed regions of meiotic prophase chromosomes. EMBO J 11, 5091–5100.
Murphy ME (2013). The HSP70 family and cancer. Carcinogenesis 34, 1181–1188.
Nakai A, Suzuki M, Tanabe M (2000). Arrest of spermatogenesis in mice expressing an active heat shock transcription factor 1. EMBO J 19, 1545–1554.
Nylandsted J, Gyrd-Hansen M, Danielewicz A, Fehrenbacher N, Lademann U, Hoyer-Hansen M, Weber E, Multhoff G, Rohde M, Jäättelä M (2004). Heat shock protein 70 promotes cell survival by inhibiting lysosomal membrane permeabilization. J Exp Med 200, 425–435.
Nylandsted J, Rohde M, Brand K, Bastholm L, Elling F, Jäättelä M (2000). Selective depletion of heat shock protein 70 (Hsp70) activates a tumor-specific death program that is independent of caspases and bypasses Bcl-2. Proc Natl Acad Sci USA 97, 7871–7876.
Okamoto T, Coultas L, Metcalf D, van Delft MF, Glaser SP, Takiguchi M, Strasser A, Bouillet P, Adams JM, Huang DC (2014). Enhanced stability of Mcl1, a prosurvival Bcl2 relative, blunts stress-induced apoptosis, causes male sterility, and promotes tumorigenesis. Proc Natl Acad Sci USA 111, 261–266.
Ollinger R, Childs AJ, Burgess HM, Speed RM, Lundegaard PR, Reynolds N, Gray NK, Cooke HJ, Adams IR (2008). Deletion of the pluripotency-associated Tex19.1 gene causes activation of endogenous retroviruses and defective spermatogenesis in mice. PLoS Genet 4, e1000199.
Paul C, Teng S, Saunders PT (2009). A single, mild, transient scrotal heat stress causes hypoxia and oxidative stress in mouse testes, which induces germ cell death. Biol Reprod 80, 913–919.
Qian SB, McDonough H, Boellmann F, Cyr DM, Patterson C (2006). CHIP-mediated stress recovery by sequential ubiquitination of substrates and Hsp70. Nature 440, 551–555.
Ravagnan L *et al*. (2001). Heat-shock protein 70 antagonizes apoptosis-inducing factor. Nat Cell Biol 3, 839–843.
Raynes DA, Guerriero V Jr (1998). Inhibition of Hsp70 ATPase activity and protein renaturation by a novel Hsp70-binding protein. J Biol Chem 273, 32883–32888.
Rockett JC, Mapp FL, Garges JB, Luft JC, Mori C, Dix DJ (2001). Effects of hyperthermia on spermatogenesis, apoptosis, gene expression, and fertility in adult male mice. Biol Reprod 65, 229–239.
Rohde M, Daugaard M, Jensen MH, Helin K, Nylandsted J, Jäättelä M (2005). Members of the heat-shock protein 70 family promote cancer cell growth by distinct mechanisms. Genes Dev 19, 570–582.
Ruggiu M, Speed R, Taggart M, McKay SJ, Kilanowski F, Saunders P, Dorin J, Cooke HJ (1997). The mouse Dazla gene encodes a cytoplasmic protein essential for gametogenesis. Nature 389, 73–77.
Russell LD, Ettlin RA, Sinha Hikim AP, Clegg ED (1990). Histological and Histopathological Evaluation of the Testis, Clearwater, FL: Cache River Press.
Sasaki T, Marcon E, McQuire T, Arai Y, Moens PB, Okada H (2008). Bat3 deficiency accelerates the degradation of Hsp70-2/HspA2 during spermatogenesis. J Cell Biol 182, 449–458.
Scieglinska D, Piglowski W, Chekan M, Mazurek A, Krawczyk Z (2011). Differential expression of HSPA1 and HSPA2 proteins in human tissues; tissue microarray-based immunohistochemical study. Histochem Cell Biol 135, 337–350.
Shaha C, Tripathi R, Mishra DP (2010). Male germ cell apoptosis: regulation and biology. Philos Trans R Soc Lond B Biol Sci 365, 1501–1515.
Shomura Y, Dragovic Z, Chang HC, Tzvetkov N, Young JC, Brodsky JL, Guerriero V, Hartl FU, Bracher A (2005). Regulation of Hsp70 function by HspBP1: structural analysis reveals an alternate mechanism for Hsp70 nucleotide exchange. Mol Cell 17, 367–379.
Son WY, Han CT, Hwang SH, Lee JH, Kim S, Kim YC (2000). Repression of hspA2 messenger RNA in human testes with abnormal spermatogenesis. Fertil Steril 73, 1138–1144.
Takayama S, Reed JC (2001). Molecular chaperone targeting and regulation by BAG family proteins. Nat Cell Biol 3, E237–241.
Turner JM, Mahadevaiah SK, Elliott DJ, Garchon HJ, Pehrson JR, Jaenisch R, Burgoyne PS (2002). Meiotic sex chromosome inactivation in male mice with targeted disruptions of Xist. J Cell Sci 115, 4097–4105.
Ulbricht A *et al*. (2013). Cellular mechanotransduction relies on tension-induced and chaperone-assisted autophagy. Curr Biol 23, 430–435.
Vos MJ, Hageman J, Carra S, Kampinga HH (2008). Structural and functional diversities between members of the human HSPB, HSPH, HSPA, and DNAJ chaperone families. Biochemistry 47, 7001–7011.
Vydra N, Malusecka E, Jarzab M, Lisowska K, Glowala-Kosinska M, Benedyk K, Widlak P, Krawczyk Z, Widlak W (2006). Spermatocyte-specific expression of constitutively active heat shock factor 1 induces HSP70i-resistant apoptosis in male germ cells. Cell Death Differ 13, 212–222.
Wang Q, Liu Y, Soetandyo N, Baek K, Hegde R, Ye Y (2011). A ubiquitin ligase-associated chaperone holdase maintains polypeptides in soluble states for proteasome degradation. Mol Cell 42, 758–770.
Widlak W, Vydra N, Malusecka E, Dudaladava V, Winiarski B, Scieglinska D, Widlak P (2007). Heat shock transcription factor 1 down-regulates spermatocyte-specific 70 kDa heat shock protein expression prior to the induction of apoptosis in mouse testes. Genes Cells 12, 487–499.
Zhu D, Dix DJ, Eddy EM (1997). HSP70-2 is required for CDC2 kinase activity in meiosis I of mouse spermatocytes. Development 124, 3007–3014.